Information flow and error scaling for fully quantum control

Stefano Gherardini [1,2,3,*] Matthias M. Müller,[4,†] Simone Montangero [5,6,7,‡] Tommaso Calarco,[4,8,§] and Filippo Caruso [2,‖]

[1]*CNR-INO, Area Science Park, Basovizza, Trieste I-34149, Italy*

[2]*Department of Physics and Astronomy & LENS, University of Florence, via G. Sansone 1, I-50019 Sesto Fiorentino, Italy*

[3]*INFN, Sezione di Firenze, via G. Sansone 1, I-50019 Sesto Fiorentino, Italy*

[4]*Peter Grünberg Institute–Quantum Control (PGI-8), Forschungszentrum Jülich GmbH, Jülich, Germany*

[5]*Dipartimento di Fisica e Astronomia "G. Galilei," Università di Padova, I-35131 Padova, Italy*

[6]*Padua Quantum Technologies Research Center, Università degli Studi di Padova*

[7]*Istituto Nazionale di Fisica Nucleare (INFN), Sezione di Padova, I-35131 Padova, Italy*

[8]*Institute for Theoretical Physics, University of Cologne, D-50937 Cologne, Germany*

(Received 31 October 2021; accepted 19 December 2021; published 11 April 2022)

The optimally designed control of quantum systems is playing an increasingly important role to engineer novel and more efficient quantum technologies. Here, in the scenario represented by controlling an arbitrary quantum system via the interaction with an another optimally initialized auxiliary quantum system, we show that the quantum channel capacity sets the scaling behavior of the optimal control error. Specifically, by fitting the model to numerical data, we verify that the minimum control error is ensured by maximizing the quantum capacity of the channel mapping the initial control state into the target state of the controlled system, i.e., optimizing the quantum information flow from the controller to the system to be controlled. Analytical results, supported by numerical evidences, are provided when the systems and the controller are either qubits or single Bosonic modes.

DOI: 10.1103/PhysRevResearch.4.023027

I. INTRODUCTION

Quantum control theory studies the steering of a quantum system from an initial state to a desired target one, by means of a control system that can be either classical or quantum [1–16]. Quantum control has played a key role in recent quantum technology breakthroughs [17–21], and, thus, the problem of identifying a universal relation for the scaling of the control error with the relevant parameters of system and control knobs is no longer only academic but also practical and even decisive for the success of any quantum platform. This especially holds if the control action is provided by the interaction between a quantum system to be controlled and an auxiliary one, namely, the quantum controller, whereby the control problem is denoted as *coherent-quantum* or *fully quantum* [22–24].

In the scenario in which a quantum system is controlled by optimal coherent pulses, which can be engineered for instance via the Krotov method [25], the gradient ascent pulse engineering (GRAPE) [26], and the (dressed) chopped random basis (dCRAB) optimal control algorithms [27–34], the cost function (or landscape), which quantifies the error in performing a desired control task, may have many local minima. This can entail the "entrapment" of the optimization procedure and, thus, the impossibility of completing the control task [7,35–37], especially in the open quantum systems case [14,38,39]. However, the situation is different when the controller is another quantum system. In this case, indeed, the control landscape, provided by the error of the control task as a function of the input state of the quantum controller, is usually convex and the optimal solution can be straightforwardly found by optimization or analytic solutions, independently of the complexity in preparing the initial state of the quantum controller [37].

A similar statement could be made about the complexity of the control action, identified by its information content. Regarding the classical control of a quantum system, it was numerically found that the control complexity has to grow at least as much as the dimension of the quantum system to be controlled [27,32,40,41]. This evidence can be even pointed out by considering the control problem as a classical communication channel between the control and the system [42,43], where the control pulse is interpreted as a communication signal whose correct reception means the complete attainment of the desired control task. Also in solving fully quantum control problems, universal results from information and communication theories could be used. In this regard, it is well-known that any physical quantum process (thus, also a quantum system interacting with a quantum controller) can be generally represented as a quantum channel that maps an initial state to a final one through a quantum dynamical map (also called quantum operation) [39].

*gherardini@lens.unifi.it
†ma.mueller@fz-juelich.de
‡simone.montangero@unipd.it
§t.calarco@fz-juelich.de
‖filippo.caruso@unifi.it

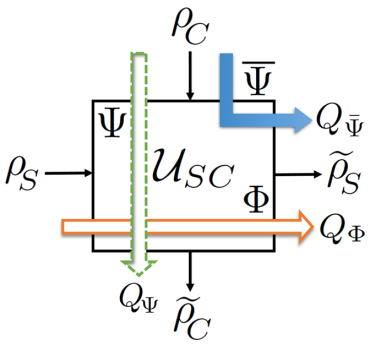

FIG. 1. Pictorial representation of a fully quantum control procedure given by the unitary interaction $\mathcal{U}_{SC}$ between the quantum system S to be controlled and the quantum controller C. The dashed green and solid orange arrows identify the channels Ψ and Φ, with quantum capacities Q_Ψ and Q_Φ, modeling the reduced dynamics of the quantum controller C and quantum system S, which map ρ_C and ρ_S into $\widetilde{\rho}_C$ and $\widetilde{\rho}_S$, respectively. The blue arrow refers to the complementary channel $\overline{\Psi}$ with quantum capacity $Q_{\bar{\Psi}}$ responsible of the quantum control performance and mapping ρ_C into $\widetilde{\rho}_S$.

In this paper, as depicted in Fig. 1, we formalize the fully quantum control problem according to the quantum channels language, commonly used in quantum information and communication theory. This allows us to determine the analytical expression of the control error scaling in reaching a desired target state. Specifically, we find that the control error scales exponentially with the quantum channel capacity of the channel linking the initial state of the controller with the output state of the controlled system (control channel). As a result, the performance of a fully quantum control is exponentially enhanced as the quantum channel capacity of the control channel increases. We provide analytical and numerical results showing how the maximization of the control channel's quantum capacity decreases the control error, when the control is optimized by properly choosing the initial state of the quantum controller. As discussed in more details below, these results are expected to find application for, among others, the state preparation of many-body quantum systems [20,21,33], the realization of photonic links [44] between quantum processors, and long-distance communication through quantum carriers [45].

II. QUANTUM CHANNELS AND CONTROL PROBLEM

Let us consider a bipartite quantum system composed of the system S to be controlled and the auxiliary one C representing the controller. The goal of the control is to bring S from the initial density operator ρ_S to the target $\hat{\rho}_S$ chosen by the user through a properly designed dynamical transformation. The latter and also the final state of the system depend on the initial (input) state ρ_C of the controller C. Here, the control problem is to find the value of ρ_C that minimizes the distance between the final and target states. To this end, the quantum controller C has to be optimally initialized.

Any physical transformation performed on a quantum system can be generally described by a family of completely positive trace-preserving (CPTP) maps $\Phi[\cdot] : \rho_S \to \widetilde{\rho}_S \equiv \Phi[\rho_S]$, with ρ_S and $\widetilde{\rho}_S$ denoting, respectively, the initial and final density operator of $\mathcal{S}$ before and after the transformation. In Fig. 1 we show a pictorial scheme identifying the fully quantum control problem given by the interaction between S and the quantum controller C. The composite system SC is initially prepared in the product state $\rho_{\rm in} = \rho_S \otimes \rho_C$, where ρ_C is denoted as the control state.

Under the assumption that the target state $\hat{\rho}_S$ belongs to the set of density operators that can be reached by the system [46], to solve the control problem we need to find the optimal value of ρ_C that allows for the equality

$$\widetilde{\rho}_S = \Phi[\rho_S] \equiv \mathrm{Tr}_C[\mathcal{U}_{SC}\,\rho_{\rm in}\,\mathcal{U}_{SC}^\dagger] = \hat{\rho}_S, \tag{1}$$

where $\mathcal{U}_{SC}$ is the unitary map describing the physical transformation of the composite system. If the target state cannot be reached by the system, the equality (1) does not have a solution and this unavoidably leads to a non zero error value ε. The control error ε is commonly expressed as a function of the Uhlmann fidelity $\mathfrak{F}(\hat{\rho}_S, \widetilde{\rho}_S) \geqslant 0$ (and $\leqslant 1$) between the target state $\hat{\rho}_S$ and the final state $\widetilde{\rho}_S$, namely, $\varepsilon = 1 - \mathfrak{F}(\hat{\rho}_S, \widetilde{\rho}_S)$, with $\mathfrak{F}(\hat{\rho}_S, \widetilde{\rho}_S) \equiv \mathrm{Tr}\sqrt{\sqrt{\hat{\rho}_S}\widetilde{\rho}_S\sqrt{\hat{\rho}_S}}$ [48]. In this case, solving the control problem corresponds to finding the optimal state ρ_C that minimizes the residual control error. Moreover, as illustrated in Fig. 1, $\Psi[\rho_C] \equiv \mathrm{Tr}_S[\mathcal{U}_{SC}\,\rho_{\rm in}\,\mathcal{U}_{SC}^\dagger]$ denotes the CPTP map that transforms ρ_C into $\widetilde{\rho}_C$, while the super-operator mapping ρ_C into $\widetilde{\rho}_S$ is given by the so-called *complementary* quantum channel that is formally defined by the map $\overline{\Psi}[\rho] : \rho_C \to \widetilde{\rho}_S$. As we will show, in the quantum control problem represented in Fig. 1, what matters to derive the error scaling behavior is our knowledge of the complementary quantum channel $\overline{\Psi}$, which depends on the initial state of the quantum system S and the way the controller C interacts with it.

III. CONTROL ERROR AND QUANTUM INFORMATION

The transmission of quantum information over a quantum channel can be quantified by the quantum capacity Q measuring the rate of information that can be reliably transmitted (thus, without any degradation) through the channel. More formally, given a set of n arbitrary quantum information carriers, the quantum capacity Q is defined as the maximum value of the ratio κ/n, where κ denotes the number of qubits employed (e.g., faithfully transmitted within a communication link) in the implemented operation [49–51]. It is worth noting that the formal derivation of Q ideally stems from the asymptotic limit of taking κ and n infinitely large, namely, by hypothetically considering unlimited resources. Therefore, being this mathematical definition an upper bound for the rate of transmitted information in a real experimental setting, usually it may not be calculated and, indeed, analytical closed formula have been found only in few cases. However, approximated values of Q can be computed by means of numerical simulations or empirical analysis [39].

Let us now translate these concepts from quantum information theory to the fully quantum control problem illustrated in Fig. 1. In doing this, we consider the complementary channel $\overline{\Psi}[\rho]$, mapping ρ_C into $\widetilde{\rho}_S$, and the corresponding quantum capacity $Q_{\bar{\Psi}}$ that quantifies the maximum rate of information needed by C to control the quantum system S. Thus, the performance in controlling S shall necessarily depend on the

value of $Q_{\bar{\Psi}}$; in this paper, we are going to investigate if there exists a formal relation expressing the error in controlling S as a function of $Q_{\bar{\Psi}}$. To evaluate this aspect, let us consider the information-theoretic error bound proposed in Ref. [42] that establishes how much a classical control action for a quantum system can be *informative*. For the sake of clarity, we here bring up a sketch of the reasoning addressed in Ref. [42] about the informativeness of a control action. In the reference, it is conjectured to ideally divide the space of possible target states $\hat{\rho}_S$ of S into hyperspheres of radius ε (called ε-balls), so that, if the final state $\widetilde{\rho}_S$ perfectly (i.e., without error) overlaps at least with one state of a given ε-ball, then any other target state in the ε-ball can be reached with a control error $\leqslant \varepsilon$. As a consequence, to "cover" all the space of possible target states by bringing the final quantum state of S over a generic target one with an error smaller than ε, the number of independent controls (equivalent to the degrees of freedom of the control) has to correspond at least to the number of ε-balls. If such requirement is satisfied, then the control action can be considered as being informative with fidelity $1-\varepsilon$. Let us note that, here, we are implicitly taking into account also the possibility that the target state $\hat{\rho}_S$ is not reachable, namely, that the equality $\widetilde{\rho}_S = \hat{\rho}_S$ cannot be achieved. What is actually important, indeed, is that the final quantum state $\widetilde{\rho}_S$ reaches the ε-ball in which the target state $\hat{\rho}_S$ is contained. By definition, the self-information associated to each ε-ball is equal to $-D\log_2(\varepsilon)$, where D denotes the dimension of the space containing the quantum states of S. This implies that, regardless of how the control procedure is implemented, classically (modulation of the system Hamiltonian via an external classical control pulse) or quantum-mechanically (see Fig. 1), the information content I_c of the control action has to be at least greater or equal to the information associated to the ε-ball:

$$I_c \geqslant -D\log_2(\varepsilon). \tag{2}$$

It follows that Eq. (2) can be interpreted as the concept that a limited amount of information encoded in the control necessarily imposes a bound on the control error. In particular, from Eq. (2) one finds that

$$-\frac{I_c}{D} \leqslant \log_2(\varepsilon) \iff \varepsilon \geqslant 2^{-I_c/D}. \tag{3}$$

According to the principles of classical and quantum information theory [39,52–54], it has been established that the information content enclosed by a given (logic, computing, communication, control, etc.) state is directly proportional to the rate with which such a state (on which, for example, a communication message is encoded) is effectively transferred. In other terms, greater is the transmission rate, and greater may be the information content carried by the transmitted state. Hence, by applying this concept to the fully quantum control problem described in Fig. 1, one gets that the information content I_c of a fully quantum control action depends on the quantum capacity $Q_{\bar{\Psi}}$ of the complementary channel $\overline{\Psi}[\rho]$. However, since by definition a quantum capacity is provided by the maximum transmission rate obtained in ideal conditions (i.e., by resorting to unlimited resources), we can state that

$$I_c \leqslant Q_{\bar{\Psi}} n, \tag{4}$$

where the further parameter n stands for the number of times the fully quantum control procedure (with reinitialization of ρ_C) is repeated, or for the number of independent quantum controllers in case the control procedure is performed only once. It is worth noting that Eq. (4) is an inequality, since in physical implementation of the fully quantum control procedure one shall expect not to recover for the information content the allowed maximum value $Q_{\bar{\Psi}} n$ due to a degradation originated by the error done in preparing the initial state of the quantum controller.

As a result, the lower bound of the fully quantum control error obeys the following relation:

$$\log_2(\varepsilon) \geqslant -\frac{Q_{\bar{\Psi}} n}{D}. \tag{5}$$

Here, we want to stress that we still do not know how tight the bound Eq. (5) is, also because so far the control error ε could have been defined also differently for this heuristic derivation. Thus, since we aim to determine a unique scaling behavior of the control error ε as a function of the quantum capacity $Q_{\bar{\Psi}}$, we introduce the parameters a_1 and a_2 that allow for the saturation of the bound, so that

$$\log_2(\varepsilon) \approx -a_1 Q_{\bar{\Psi}} - a_2. \tag{6}$$

Below, to show the effectiveness of the approximated equality Eq. (6) for the scaling of ε, some analytical examples involving a discrete and continuous variable quantum system are presented. In such cases, beyond the empirical model $-a_1 Q_{\bar{\Psi}} - a_2$, also the relations $-b_1 Q_{\bar{\Psi}}^{b_3} - b_2$ and $-c_1\log_2(Q_{\bar{\Psi}} + c_3) - c_2$ are tested, with b_k's and c_k's parameters to be fitted. A detailed numerical analysis of these three models (cf. Appendix) confirms the validity of Eq. (6) as proper scaling of ε as a function of $Q_{\bar{\Psi}}$.

IV. QUBIT-QUBIT CONTROL SCHEME

As first example, let us consider that both the system S and the controller C are qubits [55]. In this context, the reduced dynamics of C induced by system-controller interactions can be described as a map Ψ represented by only two Kraus operators [39]:

$$A_1 = \begin{pmatrix} \cos\theta & 0 \\ 0 & \cos\varphi \end{pmatrix} \quad \text{and} \quad A_2 = \begin{pmatrix} 0 & \sin\varphi \\ \sin\theta & 0 \end{pmatrix}, \tag{7}$$

such that

$$\Psi[\rho_C] \equiv \widetilde{\rho}_C = A_1\rho_C A_1^\dagger + A_2\rho_C A_2^\dagger. \tag{8}$$

This parametrization describes a wide class of two-qubit interactions as, e.g., the amplitude damping channel for $\cos(2\theta) = 1$, $\cos(2\varphi) = 2\eta - 1$ (with η damping rate), or the bit-flip channel when $\theta = \varphi$. In particular, as proved in Refs. [56–58], if $\cos(2\theta)/\cos(2\varphi) < 0$, then $Q_\Psi = 0$ and the quantum channel Ψ is denoted as antidegradable. Conversely, if $\cos(2\theta)/\cos(2\varphi) \geqslant 0$, then Q_Ψ is obtained by solving the optimization problem expressed in terms of the single-letter

formula

$$Q_\Psi = \max_{p\in[0,1]} \mathcal{S}(c_1) - \mathcal{S}(c_2), \tag{9}$$

with p a real number, $\mathcal{S}(x) \equiv -x\log_2(x) - (1-x)\log_2(1-x)$ denoting the binary Shannon entropy function, and $c_1 = p\cos^2(\theta) + (1-p)\sin^2(\varphi)$, $c_2 = p\sin^2(\theta) + (1-p)\sin^2(\varphi)$. Moreover, the quantum capacity $Q_{\bar\Psi}$ of the complementary channel $\overline{\Psi}$ can be directly derived from Q_Ψ by using the relation

$$Q_{\bar\Psi} = Q_\Psi\left(\theta \to -\overline{\theta}, \varphi \to \overline{\varphi} + \frac{\pi}{2}\right), \tag{10}$$

where

$$\widetilde{\rho}_S \equiv \overline{\Psi}[\rho_C] = \overline{A}_1\rho_C\overline{A}_1^\dagger + \overline{A}_2\rho_C\overline{A}_2^\dagger \tag{11}$$

and $\overline{A}_k \equiv A_k(\theta \to -\overline{\theta}, \varphi \to \overline{\varphi} + \frac{\pi}{2})$ with $k = 1, 2$.

According to the fully quantum control problem as defined in the previous section, we have to find the optimal control state $\rho_C = \rho_C^\star$ such that the cost function (i.e., the control error) $\varepsilon = 1 - \mathfrak{F}(\hat\rho_S, \overline{\Psi}[\rho_C]) \geqslant 0$ is minimized. Formally, for this example we can always find an analytical solution $\rho_C^\star$ such that $\widetilde{\rho}_S = \hat\rho_S$ (see the Appendix). However, only if the target state $\hat\rho_S$ is reachable by the system, the formal solution $\rho_C^\star$ corresponds to a physical state. In such a case, the quantum system S can be brought to the target state $\hat\rho_S$ with zero error. In Fig. 2, the negative logarithm of the average control error $\langle\varepsilon\rangle$ (dots)—obtained from numerical simulations—is compared with $a_1 Q_{\bar\Psi} + a_2$, both as a function of $\cos(2\overline{\theta})$ and $\cos(2\overline{\varphi}) \in [0, 1]$. For each dot plotted in Fig. 2, the average control error is computed over 1000 random target states $\hat\rho_S$, uniformly sampled from all the Bloch sphere by respecting the Haar measure [59]. The values of the parameters a_1 and a_2, instead, are determined by means of a least-squares fitting procedure. Also the maximum values $\varepsilon_{\max}$ of the control error (i.e., the respective maximum over the 1000 random target state for each set of parameters) have been analyzed: apart from a scale factor, namely, slightly different numbers of a_1 and a_2, their behavior is qualitatively comparable with the one obtained for the average values (see Fig. 4 in the Appendix). The agreement between theory and numerical simulations is very good. As discussed in the Appendix, we have tested the scaling behavior of the logarithm of the control error also by using fitting models with more than two free parameters, i.e., $-b_1 Q_{\bar\Psi}^{b_3} - b_2$ and $-c_1\log_2(Q_{\bar\Psi} + c_3) - c_2$. Overall, our analysis confirms that the average control error scales as a power of 2 proportionally to $Q_{\bar\Psi}$, as described by Eq. (6). This leads us to conclude that, apart from a few single parameter values (e.g., the limit case of $\cos(2\overline{\varphi}) \to 1$ with $\overline{\theta} \neq 0$ discussed in the Appendix), the error associated to the fully quantum control procedure follows the information-theoretical model discussed in this paper and tends to zero when the value of the quantum capacity $Q_{\bar\Psi}$ is maximized.

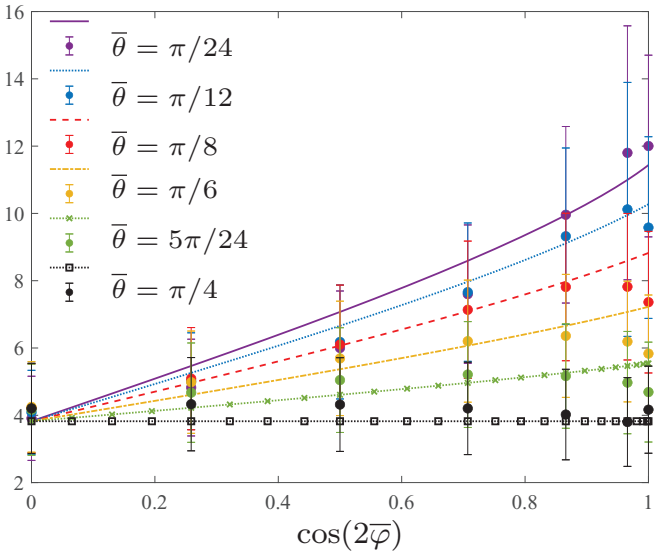

FIG. 2. Qubit-qubit control scheme. Comparison between the empirical model $a_1 Q_{\bar\Psi} + a_2$ (lines), with $Q_{\bar\Psi} \in [0, 1]$, and $-\log_2\langle\varepsilon\rangle$ (dots) as a function of $\cos(2\overline{\varphi})$ and six different values of $\cos(2\overline{\theta})$, with $\overline{\varphi}$, $\overline{\theta} = k\pi/24$, and $k = 1, \ldots, 6$. The error bars denote the standard deviation of the negative logarithm of the control error ε, while the values of the model parameters a_1 and a_2, respectively, equal to 11.8 and 3.8, are obtained by means of a single fitting procedure operating at once on all the 6 curves depicted in the figure. The average control error $\langle\varepsilon\rangle$ is obtained by solving numerically the proposed fully quantum control problem for 1000 different target states $\hat\rho_S$ and then making the average over all the sampled target states. It is worth noting that for $\cos(2\overline{\varphi}) \to 1$ with $\overline{\theta} \neq 0$ the numerical average control error slightly increases (i.e. $-\log_2\langle\varepsilon\rangle$ slightly decreases when $\cos(2\overline{\varphi})$ is very close to 1); see the Appendix for more details.

V. ONE-MODE BOSONIC GAUSSIAN CHANNELS

As second and more challenging example, S and C are taken as continuous-variable systems described in terms of one-mode Bosonic harmonic oscillators, typically a specific normal mode of the electromagnetic field. In particular, we consider the so-called Gaussian quantum channels mapping Gaussian (i.e., with a Gaussian characteristic function) input states to Gaussian output states [60] and it is experimentally widespread, since it includes not only linear attenuation and amplification processes, but also thermalization and squeezing phenomena and any physical interaction described by a quadratic Hamiltonian. As shown in Refs. [39,61], they can be described in terms of a single parameter $K \geqslant 0$ and are unitarily equivalent to two (canonical) classes of Gaussian channels, simply corresponding to attenuation and amplification processes, respectively. For $K^2 \leqslant 1$, the quantum channel corresponding to the process describes linear losses with attenuation factor K^2, while for $K^2 > 1$ an amplification with gain K^2 is obtained [39,61]. Moreover, at the level of quantum capacity, $Q_\Psi = 0$ for $K^2 \leqslant 1/2$; in such a case, the channel is called antidegradable. Otherwise, when $K^2 > 1/2$,

$$Q_\Psi = \log_2\left(\frac{K^2}{|K^2 - 1|}\right), \tag{12}$$

leading to the degradable channel case [62]. For our control purposes, also in this example the quantum capacity $Q_{\bar\Psi}$ associated to the complementary (still Gaussian) channel $\overline{\Psi}$ is determined straightforwardly from the knowledge of Q_Ψ, as in the qubit-qubit control scheme. Specifically, by means of

the functional substitution $K^2 \to 1 - \overline{K}^2$, one gets

$$Q_{\bar{\Psi}} = \log_2 \left(\frac{|1 - \overline{K}^2|}{\overline{K}^2} \right), \tag{13}$$

with $\overline{K}^2 \geqslant 0$. From here on, for the sake of simplicity of notation, we will denote $\overline{K}^2$ as q. To control the Gaussian state of the quantum system S, we need to search for the covariance matrix γ_C, associated to the control Gaussian state ρ_C, ensuring that

$$\widetilde{\gamma}_S \equiv X^T \gamma_C X + Y = \hat{\gamma}_S, \tag{14}$$

where $\hat{\gamma}_S$ is the target covariance matrix and $\widetilde{\gamma}_S$ denotes the covariance matrix of the final (Gaussian) state $\widetilde{\rho}_S$ of the system S. Note that, in doing this, we are implicitly assuming (without loss of generality) that the quantum channels Φ and Ψ are (unitarily) reduced to a canonical form, i.e., with vanishing displacements and with the matrices X and Y taking a particular symmetric form, as specified in Refs. [39,63]. Hence, $X \equiv \sqrt{q}\mathbb{1}$ and $Y \equiv |q-1|\mathbb{1}$, where $\mathbb{1}$ denotes the identity matrix, and the solution to the control problem can be analytically determined. In particular, the optimal control covariance matrix $\gamma_C^\star$, allowing for $\widetilde{\gamma}_S = \hat{\gamma}_S$ with zero error, is equal to

$$\gamma_C^\star = \begin{pmatrix} \frac{\hat{\gamma}_1 - |q-1|}{q} & \frac{\hat{\gamma}_2}{q} \\ \frac{\hat{\gamma}_2}{q} & \frac{\hat{\gamma}_3 - |q-1|}{q} \end{pmatrix} \quad \text{with} \quad \hat{\gamma}_S \equiv \begin{pmatrix} \hat{\gamma}_1 & \hat{\gamma}_2 \\ \hat{\gamma}_2 & \hat{\gamma}_3 \end{pmatrix}, \tag{15}$$

provided that $\gamma_C^\star$ obeys the generalized uncertainty relation $\gamma_C^\star \geqslant i\sigma$, where σ is the single-mode phase-space canonical symplectic matrix (taking into account all the commutation relations of the the ladder operators). If this inequality holds, then $\gamma_C^\star$ corresponds to a physical state. Otherwise, the optimal control covariance matrix is chosen as the covariance matrix that minimizes the control error $\varepsilon = 1 - \mathfrak{F}(\hat{\gamma}_S, \widetilde{\gamma}_S) \geqslant 0$, where $\mathfrak{F}(\hat{\gamma}_S, \widetilde{\gamma}_S) \equiv \mathrm{Tr}\sqrt{\sqrt{\hat{\gamma}_S}\widetilde{\gamma}_S\sqrt{\hat{\gamma}_S}}$ is the Uhlmann fidelity between the target and final covariance matrices, $\hat{\gamma}_S$ and $\widetilde{\gamma}_S$, respectively.

In Fig. 3, for $q \in [0.5, 3]$, the empirical model $a_1 Q_{\bar{\Psi}} + a_2$ is compared with the control error obtained by numerically solving the control problem for 1000 different target covariance matrices, uniformly sampled from the space of one-mode Gaussian quantum states in accordance with the Haar measure defined on this space. In particular, the numerical findings are compared with the theoretical predictions provided by the quantum capacity $Q_{\bar{\Psi}}$, the analytic curve $2^{-Q_{\bar{\Psi}}}$, and the model of Eq. (6). Also in this case, the models $-b_1 Q_{\bar{\Psi}}^{b_3} - b_2$ and $-c_1 \log_2(Q_{\bar{\Psi}} + c_3) - c_2$, defined by more than two free parameters, are tested. Similarly to the qubit-qubit control scheme, the values of the model parameters are chosen by means of a least-squares fitting procedure. We have found that the correct scaling of both the average control error $\langle\varepsilon\rangle$ (and corresponding confidence intervals defined by the error bars in Fig. 3) and the maximum values $\varepsilon_{\max}$ is reproduced by Eq. (6). The quantitative analysis of the fit, and corresponding error values, of the fitted models is presented in the Appendix. In conclusion, Fig. 3 confirms the main result discussed in this paper, namely, that for a quantum system (in this case, a continuous-variable one) the average control error, resulting by applying a fully quantum control procedure, scales exponentially as $2^{-Q_{\bar{\Psi}}}$ with the associated quantum channel capacity. Thus, the system can be potentially controlled with zero error if the capacity of the complementary channel $\bar{\Psi}$ takes its maximum value.

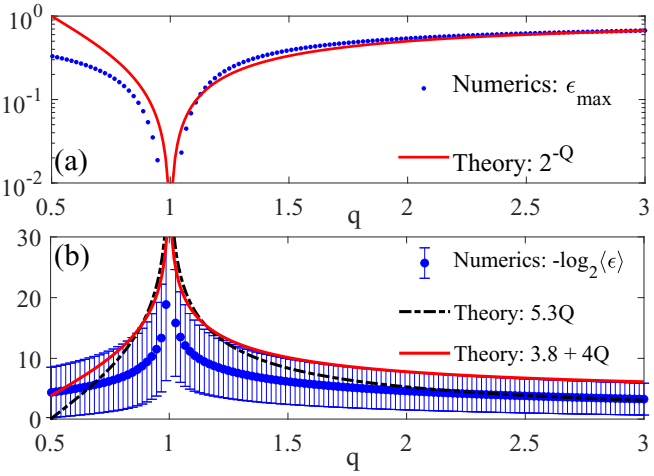

FIG. 3. Fully quantum control associated to a one-mode Bosonic Gaussian channel. (a) Comparison between the maximum values $\varepsilon_{\max}$ of the control error ε (blue dots), obtained by numerically solving the control problem for 1000 different target covariance matrices, and $2^{-Q_{\bar{\Psi}}} \equiv q/|1-q|$ (red solid line) for $q \in [0.5, 3]$ by using a logarithmic scale for the y axis (for the sake of brevity, $Q_{\bar{\Psi}}$ is denoted as Q in the legends of the two panels of the figure). Note that, although the comparison in panel (a) is more qualitative (indeed, $a_1 = a_2 = 1$), the link between $\varepsilon_{\max}$ and $Q_{\bar{\Psi}}$ can be clearly assessed. (b) Linear-scale comparison between the numerical values of $-\log_2\langle\varepsilon\rangle$ (blue dots) and the empirical model $a_1 Q_{\bar{\Psi}} + a_2$ as a function of $q \in [0.5, 3]$. While the blue dots refer to the average control error $\langle\varepsilon\rangle$ obtained by averaging ε over the sampled target covariance matrices, the blue error bars denote the corresponding standard deviations. As one can observe, there are values of a_1 and a_2 that allow for the overlap of the empirical model $a_1 Q_{\bar{\Psi}} + a_2$ with both $-\log_2\langle\varepsilon\rangle$ and the extreme points of the error bars. For the former case, the values of a_1 and a_2 are provided by the set (5.3,0) (black dotted line), while, for the latter, by the set (4,3.8) (red solid line). We have plotted both for their relevance. Finally, also notice that $Q_{\bar{\Psi}} \in [0, \infty)$: $Q_{\bar{\Psi}} = 0$ for $q = 1/2$ and $q \to \infty$, while $Q_{\bar{\Psi}} \to \infty$ when $q = 1$.

VI. APPLICATIONS

Here we identify three explicit possible applications for our results:

(i) To perform *quantum state preparation* of (many-body) quantum systems that are difficult both to access and control via classical control fields. In such cases one could use another quantum system with more control knobs as a quantum controller that allows for full control over the main system. This, for instance, may be experimentally implemented in state-of-the-art solid-state platforms exploiting nuclear spins as controller of large quantum registers of electron spins in diamond [17,64].

(ii) To realize a *photonic quantum bus* [44] being able to connect quantum memories and n-qubits quantum processors. Indeed, one could think to prepare single atoms or atomic ensemble in distinct (remote) cavities—as done, e.g., in Refs. [65–67]—and link the atoms through single photons or few-photon quantum states. Such control problem can be recast in the same class of procedures depicted in Fig. 1, whereby the atoms in the cavities represent the system S to be controlled and the photons are the quantum controller C.

(iii) To carry out *long-distance quantum communication* through flying photons [45] by implementing quantum repeater protocols, as, e.g., the one proposed by Duan-Lukin-Cirac-Zoller (DLCZ) [68]. Similarly to the previous case, pairs of entangled photons sent through the communication channel represent the auxiliary control systems, while the platforms used to realize the quantum memories of the scheme are the system that we aim to control.

VII. CONCLUSIONS

In this paper, we have analytically characterised the scaling of the error ε in controlling a quantum system S through the interaction with an auxiliary one, i.e., the quantum controller C. Specifically, we have demonstrated that ε scales as 2^{-Q_Ψ} where $Q_{\bar{\Psi}}$ is the quantum capacity of the complementary channel $\bar{\Psi}$ mapping ρ_C onto $\widetilde{\rho}_S$. These findings are confirmed by numerical simulations (Figs. 2 and 3) taking into account both discrete- and continuous-variable systems.

In all cases where the fully quantum control procedure is required, one can take the quantum controller as a quantum system with the same dimension of the controlled one and, then, optimize the control parameters with $n = 1$. Conversely, a lower-dimension controller could be employed, but one would need to choose $n > 1$, i.e., to repeat the control operation—with reinitialization of ρ_C—more than once. In any case, from the information-theoretic error scaling Eq. (5) or the empirical model Eq. (6), we can deduce that the control over a system via a quantum controller is maximized (at given quantum controller and interaction between system and controller) if the initial state of the system is chosen such that the quantum channel capacity $Q_{\bar{\Psi}}$ is maximized. This generally allows for the best possible control at the lowest possible repetitions n of the control operation. Finally, the discussed applications show the very promising impact of the achieved results on practically all the different fields involving quantum technologies.

ACKNOWLEDGMENTS

S.G., M.M.M., and F.C. acknowledge funding from the Fondazione CR Firenze through the project Q-BIOSCAN. S.G. and F.C. were financially supported from by the Fondazione CR Firenze through Project QUANTUM-AI, the European Union's Horizon 2020 research and innovation programme under FET-OPEN Grant Agreement No. 828946 (PATHOS), and from University of Florence through the project Q-CODYCES. S.G. also acknowledges The Blanceflor Foundation for financial support through the project "The theRmodynamics behInd thE meaSuremenT postulate of quantum mEchanics (TRIESTE)." M.M.M. and T.C. acknowledge funding from the European Union's Horizon 2020 research and innovation programme under Grant Agreement No. 817482 (PASQuanS), as well as from the Deutsche Forschungsgemeinschaft (DFG, German Research Foundation) under Germany Excellence Strategy—Cluster of Excellence Matter and Light for Quantum Computing (ML4Q) EXC 2004/1–390534769. S.M. kindly acknowledges support from the Italian PRIN2017 and Fondazione CARIPARO, the Horizon 2020 research and innovation programme under Grant No. 817482 (Quantum Flagship PASQuanS).

APPENDIX

1. Curve fitting of the control error

Here, we provide further details on the numerical simulations of Figs. 2 and 3. In particular, both for the qubit-qubit control scheme and the control procedure using one-mode Bosonic Gaussian channels, we will show the results obtained by numerically testing three different models for the control error scaling. In this regard, notice that for both cases the control error ε is obtained by solving the fully quantum control procedure described in the main text. Given the control error ε, the models that we have tested (below denoted as $\mathcal{M}$) by making the comparison with $-\log_2(\varepsilon)$ are the following:

(1) $\mathcal{M} = a_1 Q_{\bar{\Psi}} + a_2$,
(2) $\mathcal{M} = b_1 Q_{\bar{\Psi}}^{b_3} + b_2$,
(3) $\mathcal{M} = c_1 \log_2(Q_{\bar{\Psi}} + c_3) + c_2$.

In turn, it is worth observing that the models (i)–(iii) correspond to the following models M for the scaling behavior of ε:

(1) $M = a_3\, 2^{-a_1 Q_{\bar{\Psi}}}$ with $a_3 = 2^{-a_2}$,
(2) $M = b_4\, 2^{-b_1 Q_{\bar{\Psi}}^{b_3}}$ with $b_4 = 2^{-b_2}$,
(3) $M = c_4 (Q_{\bar{\Psi}} + c_3)^{-c_1}$ with $c_4 = 2^{-c_2}$.

Below, we will show that the scaling given by (i) [or equivalently (I)] is the best solution in terms of the fitting error $\zeta(\varepsilon)$ and/or the number of parameters adopted for the fitting. The fitting error $\zeta(\varepsilon)$ is defined as the ratio between the Euclidean distance (or L^2 norm) of the difference between $-\log_2(\varepsilon)$ and the corresponding fitting model, and the Euclidean distance $-\log_2(\varepsilon)$ alone. More formally,

$$\zeta(\varepsilon) \equiv \frac{\|\mathcal{M} + \log_2(\varepsilon)\|_2}{\|\log_2(\varepsilon)\|_2}.$$

a. Qubit-qubit control scheme

For the example with the qubit-qubit control scheme, the fully quantum control procedure requires to find the optimal value $y^\star$ and $z^\star$ of the parameters y (real number) and z (complex number) pertaining to the control state

$$\rho_C = \begin{pmatrix} y & z \\ z^* & 1-y \end{pmatrix},$$

such that $\widetilde{\rho}_S$, the final density operator of S after the control transformation, is as close as possible to the target state,

$$\hat{\rho}_S \equiv \begin{pmatrix} \hat{y} & \hat{z} \\ \hat{z}^* & 1-\hat{y} \end{pmatrix}.$$

Since $\widetilde{\rho}_S = \overline{A}_1 \rho_C \overline{A}_1^\dagger + \overline{A}_2 \rho_C \overline{A}_2^\dagger$ with $\overline{A}_1$ and $\overline{A}_2$ are the quantum maps associated to the complementary channel $\overline{\Psi}$, one can proceed to solve the equation

$$\hat{\rho}_S = \overline{A}_1 \rho_C^\star \overline{A}_1^\dagger + \overline{A}_2 \rho_C^\star \overline{A}_2^\dagger$$

as a function of the elements of the optimal control state $\rho_C^\star$ and find the analytical expressions of $y^\star$ and $z^\star$. The latter are given by the following relations:

$$y^\star = \frac{\hat{y} - \sin^2(\overline{\varphi})}{\cos^2(\overline{\theta}) - \sin^2(\overline{\varphi})},$$

$$\mathfrak{Re}\{z^\star\} = \frac{-\mathfrak{Re}\{\hat{z}\}}{\cos(\overline{\varphi} - \overline{\theta})} \quad \text{and} \quad \mathfrak{Im}\{z^\star\} = \frac{-\mathfrak{Im}\{\hat{z}\}}{\cos(\overline{\varphi} + \overline{\theta})},$$

where $\mathfrak{Re}\{x\}$ and $\mathfrak{Im}\{x\}$ denote the real and imaginary part of the generic complex number x, respectively. However, the obtained solutions are not always physically feasible. In particular, if $y^\star(1 - y^\star) - |z^\star|^2 \geqslant 0$, then the optimal control state $\rho_C^\star$ is physically realizable and one can get the equality $\widetilde{\rho}_S = \hat{\rho}_S$ with zero error. Otherwise, the optimal control state $\rho_C^\star$ is obtained as the physical state that minimizes the cost function $\varepsilon = 1 - \mathfrak{F}(\hat{\rho}_S, \widetilde{\rho}_S) \geqslant 0$, with $\mathfrak{F}(\hat{\rho}_S, \widetilde{\rho}_S) \equiv \mathrm{Tr}\sqrt{\sqrt{\hat{\rho}_S}\widetilde{\rho}_S\sqrt{\hat{\rho}_S}}$ Uhlmann fidelity. The latter is the procedure that has been followed to derive the control error ε in the numerical simulations. Specifically, ε has been computed as a function of $\cos(2\overline{\theta})$ and $\cos(2\overline{\varphi})$, both belonging to the interval [0,1], for 1000 random final target states $\hat{\rho}_S$ uniformly sampled from all the Bloch sphere by respecting the Haar measure. The negative binary logarithm of the average value of ε, i.e., $-\log_2\langle\varepsilon\rangle$, has been compared with the models (i)–(iii), all originating by the information-theoretic error bound of Eq. (5) in the main text. For all the models we now provide the values of the set of parameters $\{a_k\}_{k=1}^2$, $\{b_k\}_{k=1}^3$ and $\{c_k\}_{k=1}^3$, obtained by means of a least-squares fitting procedure, and the corresponding error values $\zeta(\langle\varepsilon\rangle)$, i.e.,

(1) $a_1 = 11.8$, $a_2 = 3.8$; $\zeta = 0.086$,
(2) $b_1 = 14.1$, $b_2 = 4.3$, $b_3 = 1.4$; $\zeta = 0.064$,
(3) $c_1 = 11.3$, $c_2 \approx 0$, $c_3 = 1.27$; $\zeta = 0.094$.

By analyzing only the error values $\zeta(\langle\varepsilon\rangle)$ (all smaller than 0.1) obtained by the fitting procedure, one can deduce that the best result is given by model (ii). However, all the error values $\zeta(\langle\varepsilon\rangle)$ are very close to each other. Thus, one can reliably state that the results from model (i) are consistent with the ones from models (ii) and (iii). Moreover, also by comparing the behavior of $-\log_2\langle\varepsilon\rangle$ as a function of $\cos(2\overline{\varphi})$ and $\cos(2\overline{\theta})$, the three models can be considered as equivalent within the relevant interval given by the values assumed by $Q_{\bar{\Psi}}$). To determine the choice of the most suitable model for the control error scaling, we resort to minimal complexity arguments, whereby the model to be privileged is the one with the lower number of free parameters/coefficients and the same fitting error. Accordingly, our choice falls on model (i) that just uses two free parameters. This confirms that the average control error scales exponentially with the negative quantum capacity $Q_{\bar{\Psi}}$. Furthermore, it is worth recalling that also the maximum values $\varepsilon_{\max}$ of the control error have been analyzed. Also in this case, as shown in Fig. 4, the scaling provided by the model (i)—comparable with the one obtained for the average values—can be observed.

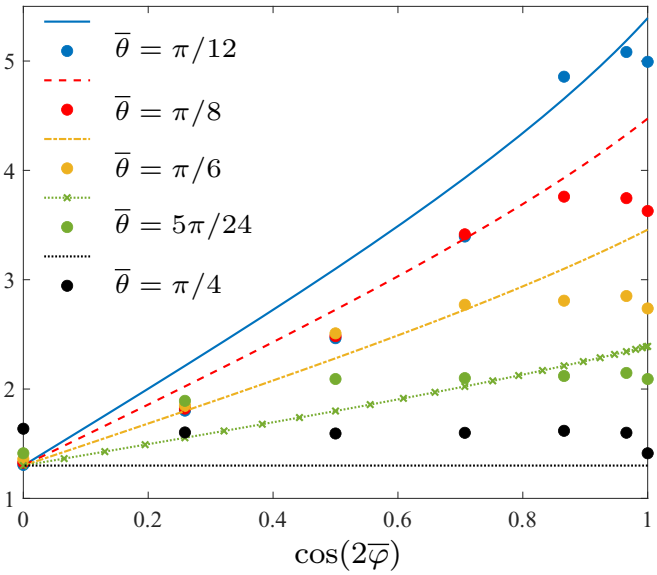

FIG. 4. Comparison between the empirical model $a_1 Q_{\bar{\Psi}} + a_2$ (lines), with $Q_{\bar{\Psi}} \in [0, 1]$, and $-\log_2 \varepsilon_{\max}$ (dots) as a function of $\cos(2\overline{\varphi})$ and five different values of $\cos(2\overline{\theta})$ corresponding to $\overline{\theta} = k\pi/24$ with $k = 2, \ldots, 6$. Again the values of the model parameters a_1 and a_2, here, respectively, equal to 7.5 and 1.3, are obtained by means of a single fitting procedure operating at once on all the five curves depicted in the figure.

Now, let us discuss more in detail the aspects regarding the increasing of the average control error $\langle\varepsilon\rangle$ (namely, the decreasing of $-\log_2\langle\varepsilon\rangle$) for $\cos(2\overline{\varphi}) = 1$ and $\overline{\theta} \neq 0$ or $\cos(2\overline{\theta}) = 1$ and $\overline{\varphi} \neq 0$. In doing this, we analyze the Kraus operators $\overline{A}_1$ and $\overline{A}_2$ that are involved in the control procedure. Such operators are equal, respectively, to

$$\overline{A}_1 = \begin{pmatrix} \cos\overline{\theta} & 0 \\ 0 & -\cos\overline{\varphi} \end{pmatrix} \quad \text{and} \quad \overline{A}_2 = \begin{pmatrix} 0 & \sin\overline{\varphi} \\ -\sin\overline{\theta} & 0 \end{pmatrix},$$

where $\overline{\theta}, \overline{\varphi} \in [0, \frac{\pi}{4}]$ so as to ensure that $Q_{\bar{\Psi}} > 0$. In particular, when $\cos(2\overline{\varphi}) = 1$ and $\overline{\theta} \neq 0$ or $\cos(2\overline{\theta}) = 1$ and $\overline{\varphi} \neq 0$, $\overline{A}_2$ becomes a singular operator and both of its eigenvalues are equal to zero. This means that, in such a case, the operator $\overline{A}_2$ is nilpotent. The singularity of the Kraus operator is the reason under the slight rising of the control error values, which in turn can be interpreted as a reduction of the dimension of the space of control states. Finally, it is also worth noting that the simultaneous validity of the conditions $\cos(2\overline{\varphi}) = 1$ and $\cos(2\overline{\theta}) = 1$, i.e., $\overline{\varphi} = \overline{\theta} = 0$, is not pathological in the sense that, apart from a phase factor, the solution to the control problem is just provided by the equality $\rho_C^\star = \hat{\rho}_S$.

b. Fully quantum control with one-mode Bosonic Gaussian channels

Any Gaussian quantum state is fully characterized by its first and second moments (of the characteristic function in the phase-space representation), also denoted as *displacement vector* and *covariance matrix*, respectively. For the fully quantum control procedure depicted in Fig. 1 in the main text, we assume that the quantum channels governing the reduced

dynamics of S and C are described as Gaussian channels, mapping Gaussian states into Gaussian ones. By applying suitable Gaussian unitaries at the input and output of the channel, one can always neglect the first moment contributions and exploit a particular symmetric form for the matrices X and Y, hence obtaining the canonical form of the channel in terms of evolution of the covariance matrix of the considered system [39]. Therefore, in our case we have to look for the covariance matrix γ_C, related to the control state ρ_C, such that

$$\widetilde{\gamma}_S \equiv X^T \gamma_C X + Y = \hat{\gamma}_S,$$

with $X \equiv \sqrt{q}\mathbb{1}$, $Y \equiv |q-1|\mathbb{1}$, q a real number greater than $1/2$, and $\hat{\gamma}_S$ being the target covariance matrix for the system state. Then, given the optimal covariance matrix $\gamma_C^\star$ provided by Eq. (15) in the main text, if the generalized uncertainty relation $\gamma_C^\star \geqslant i\sigma$ (with σ being the canonical symplectic matrix) holds, then the controller state physically exists and the control task can be carried out with zero error. Otherwise, if $\gamma_C^\star < i\sigma$, then the optimal control covariance matrix γ_C is taken so as to minimize the cost function $\varepsilon = 1 - \mathfrak{F}(\hat{\gamma}_S, \widetilde{\gamma}_S)$, with $\mathfrak{F}(\hat{\gamma}_S, \widetilde{\gamma}_S) \equiv \mathrm{Tr}\sqrt{\sqrt{\hat{\gamma}_S}\widetilde{\gamma}_S\sqrt{\hat{\gamma}_S}}$, but while satisfying the uncertainty relation $\gamma_C \geqslant i\sigma$.

On the numerical side, the control error ε is computed as a function of $q \in [0.5, 3]$ and for 1000 different target covariance matrix, uniformly sampled from the space of one-mode Gaussian quantum states in accordance with the Haar measure. Then, both the average and the maximum values of ε, $\langle\varepsilon\rangle$ and $\varepsilon_{\max}$, respectively, have been evaluated. As shown in Fig. 3(a) in the main text, the agreement between the maximum control error $\varepsilon_{\max}$ and the bound 2^{-Q_Ψ} is very good, especially for $q \in [1, 3]$. However, regarding the negative binary logarithm of the average control error $\langle\varepsilon\rangle$, we made use of the models (i)–(iii), as previously done for the qubit-qubit control scheme. The following results have been found:

(1) $a_1 = 5.3$, $a_2 \approx 0$; $\zeta = 0.36$,
(2) $b_1 = 5.3$, $b_2 \approx 0$, $b_3 = 0.64$; $\zeta = 0.14$,
(3) $c_1 = 5.16$, $c_2 \approx 0$, $c_3 = 1.1$; $\zeta = 0.27$.

The fitting procedure has been carried out by taking into account all the values of Q_Ψ pertaining to $q \in [0.5, 3]$. Instead, for each computed set of model parameters, the fitting error ζ just refer to the values of $-\log_2\langle\varepsilon\rangle$ within the interval [5,15] so as to prevent that ζ is biased by too large or too small values of the logarithm function. Thus, by analyzing the figure of merit ζ, the best results are provided by model (ii), but the values of the fitting error ζ for the models (i)–(iii) are comparable and of the same order of magnitude. For this reason and for the scaling of $-\log_2\langle\varepsilon\rangle$ in the analysed intervals, the three models can be considered consistent and with only slight differences among them. However, among the three models, only model (i) is characterized by two free parameters/coefficients, different from models (ii) and (iii) that are defined by three coefficients. Therefore, by resorting again to minimal complexity arguments, we conclude that the preferable model for the control error is the one predicted by our theoretical analysis, namely, the one provided by model (i) that has the lower number of coefficients.

[1] W. S. Warren, H. Rabitz, and M. Dahleh, Coherent control of quantum dynamics: The dream is alive, Science **259**, 1581 (1993).

[2] D. A. Steck, K. Jacobs, H. Mabuchi, T. Bhattacharya, and S. Habib, Quantum Feedback Control of Atomic Motion in an Optical Cavity, Phys. Rev. Lett. **92**, 223004 (2004).

[3] S. C. Edwards and V. P. Belavkin, Optimal quantum filtering and quantum feedback control, arXiv:quant-ph/0506018.

[4] D. D'Alessandro, *Introduction to Quantum Control and Dynamics* (Chapman & Hall/CRC, Boca Raton, FL, 2007).

[5] G. Gordon, G. Kurizki, and D. A. Lidar, Optimal Dynamical Decoherence Control of a Qubit, Phys. Rev. Lett. **101**, 010403 (2008).

[6] H. I. Nurdin, M. R. James, and I. R. Petersen, Coherent quantum LQG control, Automatica **45**, 1837 (2009).

[7] C. Brif, R. Chakrabarti, and H. Rabitz, Control of quantum phenomena: Past, present, and future, New J. Phys. **12**, 075008 (2010).

[8] H. M. Wiseman and G. J. Milburn, *Quantum Measurement and Control* (Cambridge University Press, Cambridge, UK, 2010).

[9] C. Sayrin, I. Dotsenko, X. Zhou, B. Peaudecerf *et al.*, Real-time quantum feedback prepares and stabilizes photon number states, Nature **477**, 73 (2011).

[10] C. Altafini and F. Ticozzi, Modeling and control of quantum systems: An introduction, IEEE Trans. Autom. Control **57**, 1898 (2012).

[11] F. Ticozzi, R. Lucchese, P. Cappellaro, and L. Viola, Hamiltonian control of quantum dynamical semigroups: Stabilization and convergence speed, IEEE Trans. Automatic Control **57**, 1931 (2012).

[12] F. Ticozzi, K. Nishio, and C. Altafini, Stabilization of stochastic quantum dynamics via open-and closed-loop control, IEEE Trans. Automatic Control **58**, 74 (2012).

[13] S. J. Glaser, U. Boscain, T. Calarco, C. P. Koch *et al.*, Training Schrödinger's cat: Quantum optimal control, European Phys. J. D **69**, 279 (2015).

[14] C. P. Koch, Controlling open quantum systems: Tools, achievements, and limitations, J. Phys.: Condens. Matter **28**, 213001 (2016).

[15] D. Girolami, How difficult is it to Prepare a Quantum State? Phys. Rev. Lett. **122**, 010505 (2019).

[16] S. Gherardini, F. Campaioli, F. Caruso, and F. C. Binder, Stabilizing open quantum batteries by sequential measurements, Phys. Rev. Res. **2**, 013095 (2020).

[17] T. H. Taminiau, J. Cramer, T. van der Sar, V. V. Dobrovitski, and R. Hanson, Universal control and error correction in multi-qubit spin registers in diamond, Nat. Nanotechnol. **9**, 171 (2014).

[18] M. Rossi, D. Mason, J. Chen, Y. Tsaturyan, and A. Schliesser, Measurement-based quantum control of mechanical motion, Nature (London) **563**, 53 (2018).

[19] F. Arute, K. Arya, R. Babbush, D. Bacon *et al.*, Quantum supremacy using a programmable superconducting processor, Nature (London) **574**, 505 (2019).

[20] A. Omran, H. Levine, A. Keesling, G. Semeghini *et al.*, Generation and manipulation of Schrödinger cat states in Rydberg atom arrays, Science **365**, 570 (2019).

[21] C. Song, K. Xu, H. Li, and Y.-R. Zhang *et al.*, Generation of multicomponent atomic Schrödinger cat states of up to 20 qubits, Science **365**, 574 (2019).

[22] S. Lloyd, Coherent quantum feedback, Phys. Rev. A **62**, 022108 (2000).

[23] R. J. Nelson, Y. Weinstein, and D. Cory, and S. Lloyd, Experimental Demonstration of Fully Coherent Quantum Feedback, Phys. Rev. Lett. **85**, 3045 (2000).

[24] P. Sekatski, M. Skotiniotis, and J. Kolodynski, and W. Dür, Quantum metrology with full and fast quantum control, Quantum **1**, 27 (2017).

[25] A. Konnov and V. F. Krotov, On global methods for the successive improvement of control processes, Avtomat. i Telemekh. **10**, 77 (1999).

[26] N. Khaneja, T. Reiss, C. Kehlet, and T. Schulte-Herbrüggen, and S. J. Glaser, Optimal control of coupled spin dynamics: Design of NMR pulse sequences by gradient ascent algorithms, J. Magn. Reson. **172**, 296 (2005).

[27] M. M. Müller, R. S. Said, F. Jelezko, T. Calarco, and S. Montangero, One decade of quantum optimal control in the chopped random basis, arXiv:2104.07687.

[28] P. Doria, T. Calarco, and S. Montangero, Optimal Control Technique for Many-Body Quantum Dynamics, Phys. Rev. Lett. **106**, 190501 (2011).

[29] T. Caneva, T. Calarco, and S. Montangero, Chopped random-basis quantum optimization, Phys. Rev. A **84**, 022326 (2011).

[30] S. Rosi, A. Bernard, N. Fabbri, L. Fallani, C. Fort, M. Inguscio, T. Calarco, and S. Montangero, Fast closed-loop optimal control of ultracold atoms in an optical lattice, Phys. Rev. A **88**, 021601(R) (2013).

[31] S. Hoyer, F. Caruso, S. Montangero, M. Sarovar *et al.*, Realistic and verifiable coherent control of excitonic states in a light-harvesting complex, New J. Phys. **16** (2014).

[32] N. Rach, M. M. Müller, T. Calarco, and S. Montangero, Dressing the chopped-random-basis optimization: A bandwidth-limited access to the trap-free landscape, Phys. Rev. A **92**, 062343 (2015).

[33] C. Lovecchio, F. Schäfer, S. Cherukattil, M. Alì Khan *et al.*, Optimal preparation of quantum states on an atom-chip device, Phys. Rev. A **93**, 010304(R) (2016).

[34] S. van Frank, M. Bonneau, J. Schmiedmayer, S. Hild *et al.*, Optimal control of complex atomic quantum systems, Sci. Rep. **6**, 34187 (2016).

[35] H. A. Rabitz, M. M. Hsieh, and C. M. Rosenthal, Quantum optimally controlled transition landscapes, Science **303**, 1998 (2004).

[36] B. Russell, H. A. Rabitz, and R. B. Wu, Control landscapes are almost always trap free: A geometric assessment, J. Phys. A: Math. Theore. **50**, 205302 (2017).

[37] R. B. Wu, Q. Sun, and H. A. Rabitz, Inherently trap-free convex landscapes for fully quantum optimal control, J. Math. Chem. **57**, 2154 (2019).

[38] H. Breuer and F. Petruccione, *The Theory of Open Quantum Systems* (Oxford University Press, Oxford, UK, 2003).

[39] F. Caruso, V. Giovannetti, C. Lupo, and S. Mancini, Quantum channels and memory effects, Rev. Mod. Phys. **86**, 1203 (2014).

[40] K. W. Moore and H. Rabitz, Exploring constrained quantum control landscapes, J. Chem. Phys. **137**, 134113 (2012).

[41] T. Caneva, A. Silva, R. Fazio, S. Lloyd, T. Calarco, and S. Montangero, Complexity of controlling quantum many-body dynamics, Phys. Rev. A **89**, 042322 (2014).

[42] S. Lloyd and S. Montangero, Information Theoretical Analysis of Quantum Optimal Control, Phys. Rev. Lett. **113**, 010502 (2014).

[43] M. M. Müller, S. Gherardini, T. Calarco, S. Montangero, and F. Caruso, Information theoretical limits for quantum optimal control solutions: Error scaling of noisy channels, arXiv:2006.16113.

[44] J. Simon, H. Tanji, S. Ghosh, and V. Vuletić, Single-photon bus connecting spin-wave quantum memories, Nat. Phys. **3**, 765 (2007).

[45] K. Hammerer, A. S. Sørensen, and E. S. Polzik, Quantum interface between light and atomic ensembles, Rev. Mod. Phys. **82**, 1041 (2010).

[46] For the analyzed control scheme, as given in Fig. 1, we call the system *controllable* if for any pair of initial and target states of the system there exists a physical input density operator ρ_C of the controller so that the final state of the controlled system identically equals to a given target state [47].

[47] R. Romano and D. D'Alessandro, Incoherent control and entanglement for two-dimensional coupled systems, Phys. Rev. A **73**, 022323 (2006).

[48] A. Uhlmann, The "transition probability" in the state space of a *-algebra, Rep. Math. Phys. **9**, 273 (1976).

[49] P. W. Shor, Scheme for reducing decoherence in quantum computer memory, Phys. Rev. A **52**, R2493(R) (1995).

[50] C. H. Bennett, P. W. Shor, J. A. Smolin, and A. V. Thapliyal, Entanglement-assisted capacity of a quantum channel and the reverse Shannon theorem, IEEE Transactions on Information Theory **48**, 2637 (2002).

[51] L. Gyongyosi, S. Imre, and H. V. Nguyen, A survey on quantum channel capacities, IEEE Commun. Surveys Tutor. **20**, 1149 (2018).

[52] C. E. Shannon, A mathematical theory of communication, Bell Syst. Tech. J. **27**, 379 (1948).

[53] C. E. Shannon, Communication in the presence of noise, Proc. IRE **37**, 10 (1949).

[54] T. M. Cover and J. A. Thomas, *Elements of Information Theory* (Wiley-Interscience, New York, NY, 2006).

[55] Here, the idea is to try reducing as much as possible the control complexity, so as to fulfill the control task by taking $n = 1$ and C as a qubit. In this way, the control parameters are just given by one of the elements on the diagonal of ρ_C and the real and imaginary parts of the corresponding coherence term.

[56] V. Giovannetti and R. Fazio, Information-capacity description of spin-chain correlations, Phys. Rev. A **71**, 032314 (2005).

[57] F. Caruso and V. Giovannetti, Qubit quantum channels: A characteristic function approach, Phys. Rev. A **76**, 042331 (2007).

[58] M. M. Wolf and D. Pérez-García, Quantum capacities of channels with small environment, Phys. Rev. A **75**, 012303 (2007).

[59] Note that the initial state of S is already contained in the parameters of the Kraus maps A_1 and A_2, as well as of $\overline{A}_1$ and $\overline{A}_2$. Thus, being the initial states fixed by the map, in our numerical simulations we need to randomly choose just the target states.

[60] A. S. Holevo and R. F. Werner, Evaluating capacities of Bosonic Gaussian channels, Phys. Rev. A **63**, 032312 (2001).

[61] A. Ferraro, S. Olivares, and M. G. A. Paris, *Gaussian States in Continuous Variable Quantum Information* (Bibliopolis, Napoli, 2005).

[62] F. Caruso, V. Giovannetti, and A. S. Holevo, One-mode Bosonic Gaussian channels: A full weak-degradability classification, New J. Phys. **8**, 310 (2006).

[63] A. Serafini, J. Eisert, and M. M. Wolf, Multiplicativity of maximal output purities of Gaussian channels under Gaussian inputs, Phys. Rev. A **71**, 012320 (2005).

[64] C. E. Bradley, J. Randall, M. H. Abobeih, R. C. Berrevoets, M. J. Degen, M. A. Bakker, M. Markham, D. J. Twitchen, and T. H. Taminiau, A Ten-Qubit Solid-State Spin Register with Quantum Memory up to One Minute, Phys. Rev. X **9**, 031045 (2019).

[65] B. Julsgaard, C. Grezes, P. Bertet, and K. Mølmer. Quantum Memory for Microwave Photons in an Inhomogeneously Broadened Spin Ensemble, Phys. Rev. Lett. **110**, 250503 (2013).

[66] G. Barontini, L. Hohmann, F. Haas, J. Estève, and J. Reichel, Deterministic generation of multiparticle entanglement by quantum Zeno dynamics, Science **349**, 1317 (2015).

[67] A. Morello, J. J. Pla, P. Bertet, and D. N. Jamieson, Donor spins in silicon for quantum technologies, Adv. Quantum Technol. **3**, 2000005 (2020).

[68] L.-M. Duan, M. D. Lukin, J. I. Cirac, and P. Zoller, Long-distance quantum communication with atomic ensembles and linear optics, Nature (London) **414**, 413 (2001).